

Optical Grating Recording in Highly Organized Thin Films of Disperse Red 1

*A. Miniewicz,*¹ M. Solyga,¹ H. Taunaumang,² M.O. Tija²*

¹ Institute of Physical and Theoretical Chemistry, Wrocław University of Technology, 50-370 Wrocław, Poland

² Department of Physics, Institut Teknologi Bandung, Jalan Ganesa no.10 Bandung 40132, Indonesia

Summary: Optical grating recording with submicrometer spatial resolution, which can handle grey-level patterns, has been investigated in photochromic material made of Disperse Red 1 (DR1) molecules vacuum-deposited on a glass substrate. Holographic gratings of periods Λ within the range of 0.6 μm - 12 μm were recorded by 514.5 nm light from cw Ar^+ laser using a degenerate two-wave mixing technique. Despite the very small DR1 layer thickness ($\sim 0.1 \mu\text{m}$), the diffraction efficiency measured in a Raman-Nath scattering regime reached 2 %. The obtained amplitude gratings were analysed with an optical microscope and Fourier transforms. Grating profiles were analysed in relation to exposure conditions and in correlation with molecular organisation. Polarising microscopy studies revealed the presence of light-induced optical anisotropy. Following that, we have checked the possibility of polarisation-sensitive recording in this medium.

Keywords: Disperse Red 1; grating recording; holographic materials; photochromism

Introduction

Properties of polymers containing photochromic azo dyes have received enormous attention. These materials could be suitable for applications in photonics, e.g. as holographic optical elements or 3-D data storage media [1-5]. Except polymers, a thin highly organised film of organic compounds can be envisaged for dense 2-D optical holographic storage of information providing their properties could be permanently and/or reversibly modified by laser light. Thin molecular layers of thickness of the order of 0.1 μm provide high spatial resolution suitable for holographic recording in a small-size region ($\sim 100 \mu\text{m}$). One of the already known methods of

producing such films is the physical vacuum deposition (PVD) technique. Using PVD with an option of heated substrate, the highly oriented thin layers of low-molecular-weight organic materials like DMANS ((dimethylamino)nitrostilbene) and p-NA (4-nitroaniline) were deposited [6-8]. Taunamang et.al. [9] confirmed by x-ray, FTIR and other spectroscopic techniques that 4-[ethyl(2-hydroxyethyl)amino]-4-nitroazobenzene known as Disperse Red 1 (DR1), when evaporated on glass, Si or ITO-covered glass, can form highly organised molecular layers with molecules standing almost perpendicular to the surface. It is well known that molecules of DR1 embedded in polymer matrices can be easily switched by light between their two stable forms, *trans* and *cis*. This phenomenon should not occur in densely packed media due to the lack of free space around the molecule to permit the transition of *trans*-form into the bent *cis*-form of DR1. In our preceding paper, we investigated whether optical grating recording with 514.5 nm laser light is possible in highly organised layers of pure DR1 [10] and we have found that absorption-type gratings can be recorded. In this report, we would like to focus our attention on spatial resolution achievable in such a medium and, by discovering the possibility of polarisation grating recording, to shed more light on molecular mechanism responsible for the observed effects.

Experimental

DR1 with molecular mass 314.3 and melting point at 153 °C was obtained from Sigma. The DR1 thin films were evaporated onto glass and ITO-covered glass substrates under vacuum $(2.7-4) \times 10^{-3}$ Pa with crucible temperature kept at 173 °C. The temperature of the substrate was kept at 26 °C. After evaporation, no further annealing was performed. The layer thickness was determined with a Dektak IIA depth profilometer giving values of 0.07 – 0.1 μm . Crystallinity of the obtained layers was examined with an X-ray Philips diffractometer ($\lambda = 1.5406 \text{ \AA}$). The most pronounced diffraction peak corresponded to an interlayer distance of 9.8 \AA , which is close to the length of DR1 molecule in its elongated *trans* form. These and other investigations (FTIR, RAS FTIR) of molecular ordering [9] are consistent with the assumption that the PVD of DR1 on glass leads to near perpendicular long-molecular-axis alignment with respect to the substrate plane. It was also demonstrated that when during the PVD process substrates are kept at higher temperatures (55 and 75 °C), both the crystallinity and ordering increase [9]. Refraction index of the as-grown films measured by the standard prism coupling technique amounted to $n = 1.508$.

Results

Absorption spectra in the visible spectral region, shown in Fig. 1, exhibit a sharp peak at around 400 nm assigned to the formation of J-type or H-type molecular aggregates. Linear absorption coefficient estimated from the spectrum and direct light attenuation measurements at 514.5 nm, with the assumption of layer thickness $d = 0.1 \mu\text{m}$, amounts to $\alpha \cong 40000 \text{ cm}^{-1}$.

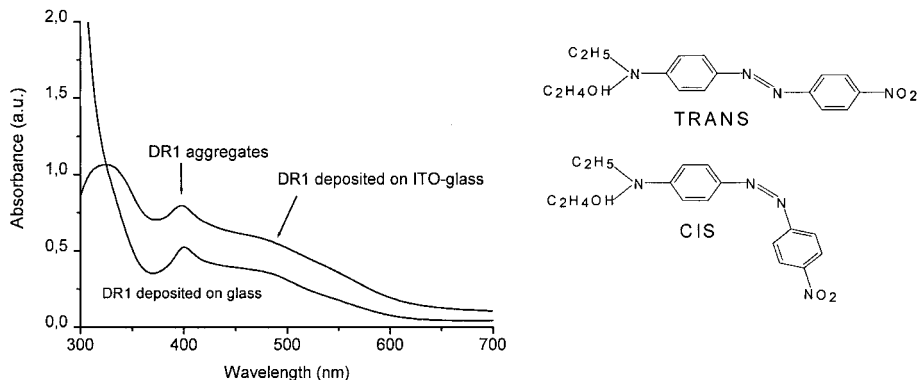


Figure 1. Absorption spectra of 0.1 μm thick layers of DR1 deposited by the PVD method on glass plate and ITO-covered glass plate kept at 26 °C during evaporation. On the right: *trans* and *cis* forms of the DR1 photoisomers are shown.

In the prepared DR1 layers, we recorded gratings using the standard holographic technique of two-wave mixing with an Ar⁺-ion laser (Innova 90, Coherent) working at 514.5 nm wavelength. The technique was modified for the purpose of the present studies by introduction of a lens giving small spots of 294 or 167 μm in diameter measured at $1/e^2$ ($e = 2.718$) of the maximum intensity of a Gaussian beam at the center. The experimental set-up is shown in Fig. 2a. We used TEM₀₀ Gaussian beam with rotationally symmetric amplitude distribution given by $A(\rho) = A_0 \exp(-\rho^2 / w^2)$ and $I(r) = \frac{1}{2} \epsilon_0 c n |A(r)|^2$ where ρ is the cylindrical coordinate perpendicular to the direction of propagation z and w is the spot size. In the grating recording experiment, the intensity distribution $I(x)$ is periodically modulated and described by the relation:

$$I(x) = I_1 + 2\Delta I \cos(Kx) + I_2 \quad (1)$$

where $K = 2\pi/\Lambda$ is the grating wave vector and $\Delta I = \frac{n}{2} \varepsilon_0 c A_1 A_2^*$. In order to account for the cases

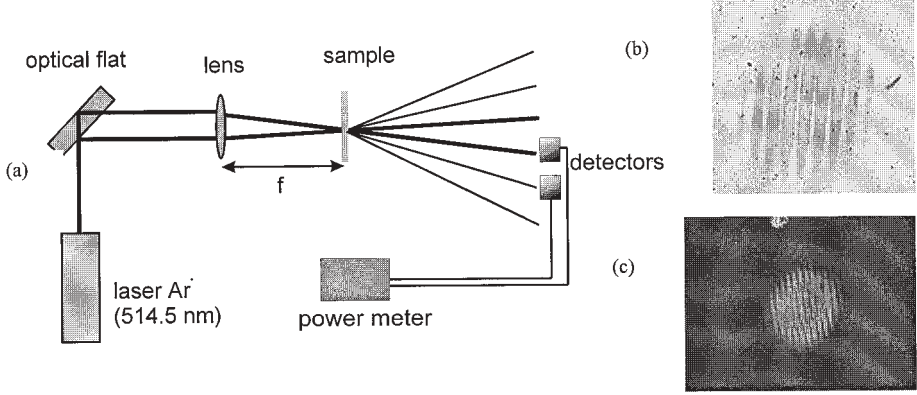


Figure 2. Experimental set-up for optical recording of gratings in DR1 layers deposited on glass. Measurements of 0th- and 1st-order diffraction intensities were made with a Labmaster Ultima (Coherent Inc.), two-channel power meter (a). Photographs of gratings under microscope (b) and under crossed-polarisers condition (c).

of grating recording in the media with anisotropic interaction, one defines $\Delta I = \left| \text{tr} \{ \Delta M_{ij} \} \right|$, where the ΔM_{ij} is the interference tensor. In the s:s (VV) polarisation experiment, $\Delta I = \sqrt{I_1 I_2}$ while for the s:p (VH) configuration, $\Delta I = 0$ and there is no light intensity modulation along the x -direction (grating wavevector). In a typical experiment with $P_1 = 4.72$ mW, $P_2 = 3.28$ mW, modulation factor $m = 0.98$ and average light intensities at the fringe centres were 23 W/cm^2 and 72 W/cm^2 for $f_1 = 450$ mm and $f_2 = 255$ mm lenses, respectively. So recorded gratings in DR1 layers were permanent. Experimental diffraction efficiencies η were determined as the ratio of the power diffracted into first-order direction (P_{diff}) and the transmitted beam power (P_t), $\eta = \frac{P_{\text{diff}}}{P_t}$. From

the value of Klein's parameter $Q = 0.0007$ ($Q = \frac{2\pi\lambda d}{n\Lambda^2}$, $\lambda = 0.5145 \mu\text{m}$, $n = 1.508$, $\Lambda = 17 \mu\text{m}$, and $d = 0.1 \mu\text{m}$) it follows that we are in the Raman-Nath scattering regime of thin gratings. The transmittance of a thin grating can be expressed by the relationship $t(x) = \exp(\alpha(x)d)\exp(-ikdn(x))$ where $\alpha(x)$ and $n(x)$ are the x distributions of the index of absorption and index of refraction, respectively. An example of a microscopic image of a grating recorded in the DR1 film vacuum-deposited on glass is given in Fig. 2b ($\Lambda = 17 \mu\text{m}$). In the bright regions of the interference fringes, the absorption is increased compared with unilluminated areas. The grating profile in its central part can roughly be described by $\alpha(x) = \alpha_{av} + \Delta\alpha(1 + \sin(Kx))$ where $\alpha_{av} = 40000 \text{ cm}^{-1}$ is the average absorption coefficient of the layer outside the illuminated region and $\Delta\alpha$ is the amplitude of the absorption grating to be determined. From the Kramers-Kronig relations [11], it is known that any modulation of absorption coefficient in a material is accompanied by the respective modulation of its refractive index $n(x) = n_{av} + \Delta n(1 + \sin(Kx))$. This is the reason why we assumed the coexistence of the amplitude $\Delta\alpha$ and the phase Δn gratings in the layer. The observation of the grating area under the condition of crossed polarisers (cf. Fig. 2c) evidences that the illuminated region becomes, as a whole, optically anisotropic. In that region the light polarization is rotated. This experiment tells us that the virgin DR1 layer is optically isotropic (molecules are either completely disordered or stand almost perpendicularly to the glass surface). However, an increase in absorption upon illumination supports the assumption that initially the molecules were more or less perpendicular to the layer. The coloration indicates that the illuminated regions become more absorptive, i.e., the average molecular angle measured with respect to the surface decreases from 90° to lower values. The reason can be heat-induced oriented crystallite growth (of sizes $s \ll \lambda$) or concerted tilt and reorientation of the molecules similar to those observed in polymer matrices [1-5]. The prolonged illumination with an intense focused light ($\lambda = 514.5 \text{ nm}$) eventually leads to the film degradation at the centre (sublimation of DR1) with microscopic crystallites appearing around the centre of the beam spot. This observation supports the heat-induced oriented-crystallite growth mechanism as the one responsible for the absorption grating formation.

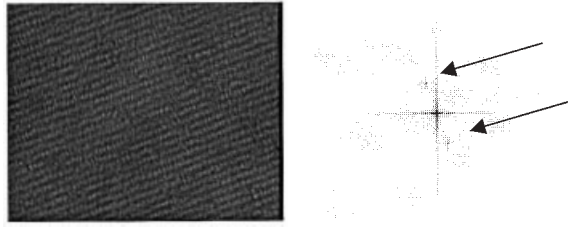


Figure 3. Photograph of the amplitude grating recorded with a period of $0.59\ \mu\text{m}$ made with an optical microscope and its Fourier transform showing a single period (cf. two spots around the centre of the Fourier spectrum).

In Fig. 3 we show that recording a very dense grating with period $\Lambda = 0.59\ \mu\text{m}$ is possible. The observation of such a high-frequency grating is close to the resolution limit of our optical microscope (Olympus BX 60), but the Fourier transform of the grating shows the well defined single period (cf. spots in the Fourier transform spectrum). Depending on the exposure, the profiles of absorption gratings change dramatically. In Fig. 4, the Fourier transform of the properly exposed grating shows only one Fourier component whereas overexposed grating shows up to three Fourier components indicating a severely distorted sinusoidal profiles.

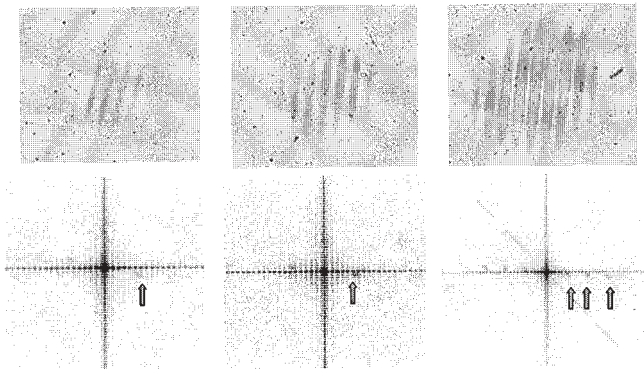


Figure 4. Gratings formed at different exposures and their Fourier transforms. Overexposure causes that the grating shows more than one Fourier component.

A closer inspection of the grating profiles (various cross-sections) obtained for a long-exposure grating is shown in Fig. 5. A bleaching in the central part of the grating and a nonsinusoidal shape of the fringes (cf. Fig. 5a) are noticeable while well sinusoidal fringes and no bleaching is observed for a section outside the central part (cf. Fig. 5b).

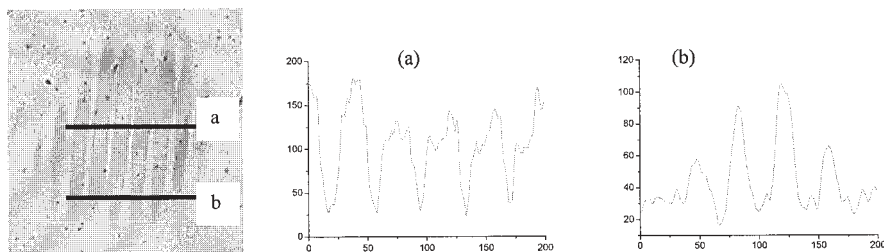


Figure 5. The sections along the grating showing a change in absorption grating profiles as a function of place, i.e. intensity level during recording process.

Kinetics of grating recording in DR1 layers

The kinetics of grating recording has been measured by monitoring the first-order diffraction power with respect to the exposure. The time evolution of the first-order diffraction efficiency (cf. Fig. 6) behaves totally differently when compared with grating recording experiments measured with chromophore-doped polymers where exponential growth with saturation is usually observed. In the case of thin DR1 layers, one observes the well-defined maximum of diffraction efficiency η followed at higher exposures by a minimum and subsequent maximum. Tentative explanation of such a behaviour must take into account the Gaussian distribution of intensity, which causes non-uniformity of the recorded grating amplitude across the grating area and the very limited number of fringes.

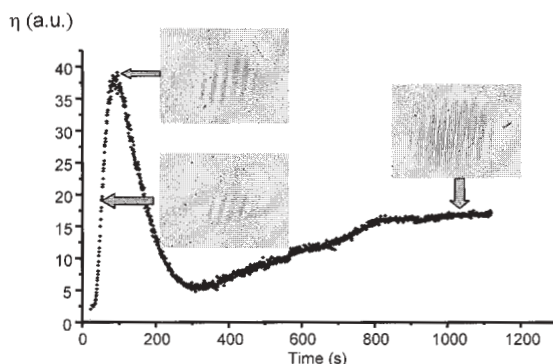


Figure 6. Time evolution of the first-order diffraction efficiency together with photos of gratings created at the marked points [10].

Thus, initially at the beam centre ($\rho = 0$), the grating amplitude grows faster due to higher incoming light intensity. The molecules are tilted and the amplitude of absorption grating reaches its maximum at the moment when the grating is perfectly sinusoidal with the maximum attainable amplitude, $\Delta\alpha_{\max}$. This effect is well documented in Fig. 6 where the photographs of the gratings recorded in the DR1 film are shown. The decrease in diffraction efficiency might be associated with bleaching of the absorption in the vicinity of each fringe and in the whole central part of the grating. Grating evidently becomes less sinusoidal, so the diffraction in the first-order direction competes now with the diffraction into higher diffraction orders. The mechanism which is responsible for the subsequent rise in diffraction efficiency may originate from (i) slow rise in the first-order diffraction coming from side parts of the beam centre where the grating is still sinusoidal and (ii) slow but progressive mechanism associated with sublimation of the molecules. Due to this process, the material becomes again more transparent and more diffracted light can be collected with a detector placed in the first-order diffraction direction. All these processes are difficult to model. However, the indirect evidence that the above mentioned scheme may be realistic is given by the following experiment of grating recording without lenses and with a very short grating period $\Lambda = 0.6 \mu\text{m}$. In this case, due to lower total light intensity, sublimation, bleaching and side effects are limited and the kinetics of the first-order diffraction power resemble those measured in typical photochromic materials (cf. Fig. 7, VV grating recording).

Grating translation studies [12,13] as well as microscopic observations allowed to determine the ratio of amplitude ($\Delta\alpha$) and phase (Δn) grating strengths at the maximum of diffraction efficiency $\Delta\alpha / \Delta n \cong 7.2 \times 10^{-5} \text{ cm}^{-1}$. From these data one can estimate the contribution to the overall diffraction efficiency, $\eta_{\text{tot}} = 1.57 \%$, coming from the refractive index grating, $\eta_{\Delta n} = 6.5 \times 10^{-2} \%$. Thus one can state that the contribution of pure phase grating to the observed diffraction is about 25 times lower than the contribution of pure absorption grating at 514.5 nm.

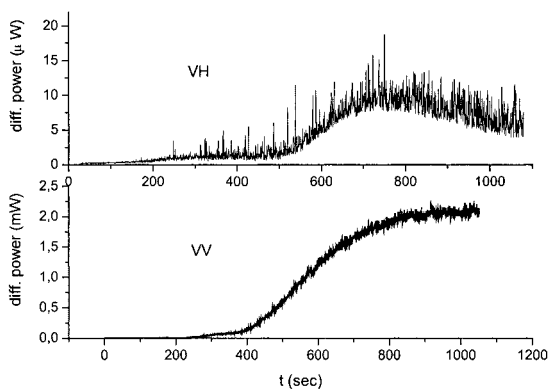


Figure 7. Examples of polarisation (VH) and intensity (VV) grating recording in DRI layer without focusing the writing beams ($\Lambda = 0.6 \mu\text{m}$).

In Fig. 7 we show for the first time, to our knowledge, the formation of the polarisation grating in a highly ordered film of DRI molecules on glass. Two recording beams were carefully orthogonally polarised with respect to each other. Polarisation grating (VH) written under the same laser power conditions as the intensity grating (VV) gives a much smaller diffraction power, 10 μW versus 2 mW. Note that under a lower light intensity than that used previously, the “incubation” time of grating formation is much longer and the characteristics of grating dynamics are different.

Conclusions

We investigated the process of holographic absorption grating recording in thin layers of Disperse Red 1 vacuum-deposited on glass substrate. We observed a relatively high self-diffraction efficiency at 514.5 nm reaching at the best 2 % for a 100-nm thick DR1 layer. The spatial resolution reaches 2000 lines/mm. From the presented results, we postulated the mechanism of photoinduced grating formation in highly organized thin films of DR1. Molecules during grating recording are addressed with strongly absorbed light and, due to local heating and/or *cis-trans* multiple excitations, change their initial orientation producing stronger absorption in the illuminated regions. The molecular reorientation is not completely random as it produces optical birefringence. The process is well controlled by experimental conditions, i.e., the growth rate depends on the light illumination level in a highly predictable manner.

Acknowledgements

A part of this work was supported by the Polish State Committee for Scientific Research under grant 4T 08A 03523.

- [1] M. S. Ho, A. Natansohn, and P. Rochon, *Macromolecules* **1995**, 28, 6124.
- [2] Z. Sekkat, J. Wood and W. Knoll, *J. Phys. Chem.* **1995**, 99, 17226.
- [3] T.G. Pedersen, P.M. Johansen, N.C.R. Holme, P. Ramanujam, S. Hvilsted, *J. Opt. Soc. Am. B* **1998**, 15, 1120.
- [4] P.-A. Blanche, P.C. Lemaire, C. Maertens, P. Dubois, R. Jerome, *Opt. Commun.* **2000**, 185, 1.
- [5] P. Lefin, C. Fiorini, J-M. Nunzi, *Opt. Mater.* **1998**, 9, 323.
- [6] T. Kaino, A. Yokoo, M. Asabe, S. Tomaru, T. Kurihara, *Nonlinear Opt.*, **1995**, 14, 135.
- [7] T. Ehara, H. Hirose, H. Kobayashi, M. Kotani, *Synth. Met.*, **2000**, 109, 43.
- [8] N. Okamoto, H. Unoh, O. Sugihara, R. Matsushima, *Nonlinear Opt.*, **1995**, 14, 245.
- [9] H. Taunaumang, Herman, M.O. Tija, *Opt. Mater.* **2001**, 18, 343.
- [10] H. Taunaumang, M. Solyga, M.O. Tija, A. Miniewicz, *Opt. Mater.*, submitted
- [11] H.J. Eichler, P. Guenter, D.W. Pohl, *Laser-Induced Dynamic Gratings*, Springer, Berlin **1986**, pp. 98-99.
- [12] K. Sutter, P. Gunter, *J. Opt. Soc. Am. B.* **1990**, 7, 2274.
- [13] C.H. Kwak, A.J. Lee, *Opt. Commun.*, **2000**, 183, 547.